Electrocatalysts Hot Paper

DOI: 10.1002/ange.201307203

Carbon Nanotubes/Heteroatom-Doped Carbon Core–Sheath Nanostructures as Highly Active, Metal-Free Oxygen Reduction Electrocatalysts for Alkaline Fuel Cells**

*Young Jin Sa, Chiyoung Park, Hu Young Jeong, Seok-Hee Park, Zonghoon Lee, Kyoung Taek Kim, Gu-Gon Park, and Sang Hoon Joo**

Abstract: *A facile, scalable route to new nanocomposites that are based on carbon nanotubes/heteroatom-doped carbon (CNT/HDC) core–sheath nanostructures is reported. These nanostructures were prepared by the adsorption of heteroatom-containing ionic liquids on the walls of CNTs, followed by carbonization. The design of the CNT/HDC composite allows for combining the electrical conductivity of the CNTs with the catalytic activity of the heteroatom-containing HDC sheath layers. The CNT/HDC nanostructures are highly active electrocatalysts for the oxygen reduction reaction and displayed one of the best performances among heteroatom-doped nanocarbon catalysts in terms of half-wave potential and kinetic current density. The four-electron selectivity and the exchange current density of the CNT/HDC nanostructures are comparable with those of a Pt/C catalyst, and the CNT/HDC composites were superior to Pt/C in terms of long-term durability and poison tolerance. Furthermore, an alkaline fuel cell that employs a CNT/HDC nanostructure as the cathode catalyst shows very high current and power densities, which sheds light on the practical applicability of these new nanocomposites.*

The oxygen reduction reaction (ORR) is a ubiquitous reaction and plays a pivotal role in the overall performance of electrochemical energy devices, such as fuel cells[1] and metal–air batteries.[2] Platinum-based electrocatalysts have been predominantly used for the ORR; however, they exhibit sluggish kinetics for the ORR and declining activity with long-term use. Furthermore, the very high cost of platinum, combined with its scarcity, has further hampered the widespread use of these fuel cell systems. Hence, tremendous effort has been geared towards the development of highly active and stable, yet low-cost ORR electrocatalysts that are based on compositions with a low platinum content or no platinum at all.[3–6] Among such classes of catalysts, nanocarbons doped with heteroatoms have shown highly promising ORR activity, particularly in alkaline media.[6] Over the last few years, various carbon nanostructures, including carbon nanotubes,[7,8] graphene,[9,10] nanoporous carbons,[11] and carbon nitrides,[12] that were doped with various heteroatoms have been exploited as electrocatalysts for the ORR in alkaline media. Despite this rapid progress, there still remains a multitude of challenges in the development of doped nanocarbon-based electrocatalysts. First, the preparation of doped carbon nanostructures, particularly carbon nanotubes and graphene, is predominantly achieved by in situ doping by chemical vapor deposition (CVD) or annealing of pure carbon materials under reactive gas; however, these methods are unfavorable for large-scale syntheses and unavoidably involve the use of toxic gases, such as ammonia or acetonitrile. Second, the ORR activity of doped carbon nanostructures is still inferior to that of Pt/C catalysts; Pt/C catalysts generally show a half-wave potential of approximately 0.80–0.90 V (vs. the reversible hydrogen electrode

[*] Y. J. Sa,[+] Dr. C. Park,[+] Prof. K. T. Kim, Prof. S. H. Joo
Department of Chemistry and School of Nano-Bioscience and Chemical Engineering
Ulsan National Institute of Science and Technology (UNIST)
Ulsan 689-798 (Republic of Korea)
E-mail: shjoo@unist.ac.kr
Homepage: http://shjoo.unist.ac.kr/

Y. J. Sa,[+] Prof. S. H. Joo
KIER-UNIST Advanced Center for Energy, UNIST
Ulsan 689-798 (Republic of Korea)

Dr. H. Y. Jeong, Prof. Z. Lee
School of Mechanical and Advanced Materials Engineering and Low-Dimensional Carbon Materials Center, UNIST
Ulsan 689-798 (Republic of Korea)

Dr. H. Y. Jeong
UNIST Central Research Facility, UNIST
Ulsan 689-798 (Republic of Korea)

Dr. S.-H. Park, Dr. G.-G. Park
Fuel Cell Research Center, Korea Institute of Energy Research
Daejeon 305-343 (Republic of Korea)

[+] These authors contributed equally to this work.

[**] This work was supported by the National Research Foundation (NRF) of Korea, which is funded by the Ministry of Education (NRF-2013R1A1A2012960 to S.H.J. and NRF-2013R1A1A2063049 to C.P.), the 2012 Future Challenge Research Fund (1.130014) of UNIST, and the Research and Development Program of the Korea Institute of Energy Research (B4-2423). S.H.J. was supported by the New & Renewable Energy Core Technology Program of the Korea Institute of Energy Technology Evaluation and Planning (KETEP) funded by the Ministry of Trade, Industry & Energy (20133030011320). Z.L. acknowledges the Nano Material Technology Development Program through the NRF funded by the Ministry of Science, ICT, and Future Planning (2012M3A7B4049807). Y.J.S. is thankful for a Global Ph.D. Fellowship (NRF-2013H1A2A1032644). We are grateful to Prof. Liming Dai for helpful discussions.

Supporting information for this article is available on the WWW under http://dx.doi.org/10.1002/anie.201307203.

 © 2014 Wiley-VCH Verlag GmbH & Co. KGaA, Weinheim

(RHE)), whereas the half-wave potential of doped carbon nanostructures ranges from 0.60 to 0.80 V (vs. RHE). Finally, the application of doped carbon nanostructures in alkaline fuel cells, which is critical to their practical use, has rarely been demonstrated.[13]

Herein, we report an ionic liquid (IL)-driven, facile, scalable route to new carbon nanostructures that comprise pure CNT cores and heteroatom-doped carbon (HDC) sheath layers for the first time. The CNT/HDC nanostructures show excellent electrocatalytic activity for the ORR, which was confirmed by their very high half-wave potential and kinetic current density in alkaline media. To the best of our knowledge, the ORR activity of these CNT/HDC nanostructures is one of the best performances among all heteroatom-doped nanocarbon catalysts. The kinetic parameters of the CNT/HDC nanostructures compare favorably with those of a Pt/C catalyst. The CNT/HDC nanostructures also exhibit superior long-term durability and poison tolerance compared to Pt/C. Furthermore, the CNT/HDC nanostructures show very high current and power densities when employed as the cathode catalyst in an alkaline fuel cell.

The procedure for the synthesis of the CNT/HDC core–sheath nanostructures is illustrated in Scheme 1. ILs were selected as precursors for the formation of the HDC layers

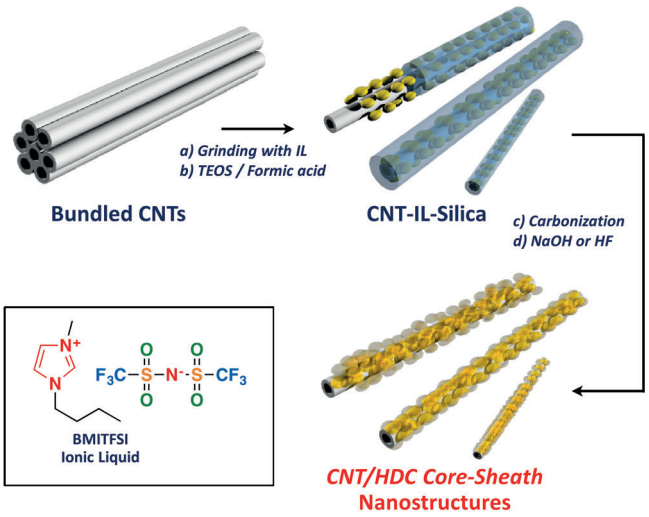

Scheme 1. Synthesis of the CNT/HDC core–sheath nanostructures.

because of their versatility as environmentally benign sources for carbon nanostructures[14] as well as their atomic composition with various heteroelements (for detailed procedures, see the Supporting Information). We began by producing a monolithic gel of a CNT–IL–silica composite using multi-walled CNTs, an IL [1-butyl-3-methylimidazolium bis(trifluoromethylsulfonyl)imide (BMITFSI)], and a silica source [tetraethyl orthosilicate (TEOS)]. The CNTs were heated with acid at reflux to remove metallic impurities prior to formation of the composite. By grinding the CNT powder with BMITFSI, the CNTs were exfoliated,[15] and the mixture became a black paste-like gel. The subsequent addition of TEOS and formic acid resulted in the formation of a CNT–IL–silica composite monolith after several hours. Subsequent carbonization at a desired temperature of 800 °C to 1000 °C, followed by the etching of silica afforded CNT/HDC-*X* (*X* = carbonization temperature) nanostructures. In the absence of CNTs, this procedure yielded HDC nanostructures. BMITFSI contains nitrogen atoms in the imidazolium cations and nitrogen, sulfur, and fluorine atoms as part of the anions; these elements can therefore serve as heteroatom sources in the HDC sheath layer.

The formation of the CNT/HDC nanostructures was observed by transmission electron microscopy (TEM; Figure 1 a, b; see also the Supporting Information, Figure S1). An atomic resolution (AR) TEM image of the CNTs reveals the atomic structure of the CNTs, which are composed of three to

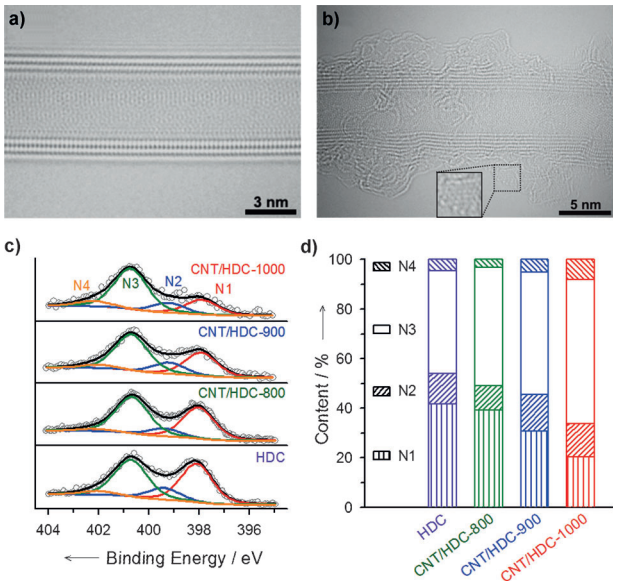

Figure 1. a, b) AR-TEM images of CNTs (a) and CNT/HDC-1000 (b). c) N 1s XPS spectra of the HDC and CNT/HDC nanostructures. d) Relative ratios of the deconvoluted peak areas of the N 1s XPS spectra.

eight multi-walls with an outer diameter of approximately 5–10 nm (Figure 1 a). The AR-TEM image of CNT/HDC-1000 clearly confirms the successful formation of rough sheath layers on the CNT walls (Figure 1 b). The HDC sheaths were in close contact with the walls of the pristine CNTs, and their thickness was measured to be 1–5 nm. Remarkably, the HDC sheaths have graphitic structures, as clearly confirmed by a hexagonal lattice image (Figure 1 b, inset). The composition and structure of the CNTs and the CNT/HDC nanostructures were assessed with X-ray photoelectron spectroscopy (XPS). The XPS survey spectrum of the CNTs showed a pronounced C 1 s peak and a trace peak for O 1 s, which confirmed that the CNTs were free of metals after the acid pre-treatment (Figure S2). Noticeable changes after formation of the HDC sheath layer on the CNTs were the appearance of new peaks, which correspond to heteroatoms, at 400 eV (N 1 s), 165 eV (S 2 p), and 690 eV (F 1 s) and an increase in the intensity of the peak at 530 eV (O 1 s; Figure 1 c and S2–S4), indicating the formation of HDC sheath layers with three different (N, S,

 © 2014 Wiley-VCH Verlag GmbH & Co. KGaA, Weinheim

and F) dopants. More detailed analyses of the N 1s XPS spectra of the CNT/HDC nanostructures and HDC are presented in Figure 1c and Table S1. The N 1s peaks of the samples were deconvoluted into four peaks at 398.0 eV, 399.3 eV, 400.7 eV, and 402.1 eV, which could be assigned to pyridinic (N1), pyrrolic (N2), graphitic (N3), and N–O (N4) nitrogen species, respectively.[9b] Whereas the position of each peak was preserved on heating, the relative ratios of the peaks changed significantly.

Notably, the area of the peak that corresponds to the graphitic nitrogen atom increased gradually with increasing annealing temperature, whereas that of the pyridinic nitrogen atom decreased. Furthermore, the peak area of the N–O species also increased with temperature, which may be suggestive of stronger interactions of the surfaces of the CNT/HDC nanostructures with oxygen. Detailed XPS quantitative analysis of the respective elements (Table S2) revealed that the total amount of the heteroatoms (N, S, and F) in the CNT/HDC nanostructures decreased from 8.8 wt% to 6.6 wt% with an increase in temperature. Raman spectra of the CNT/HDC nanostructures featured a pronounced, graphitic G band and negligible, disordered D band peaks, which indicates that the CNT nanostructures preserve a highly graphitic character even after the functionalization with HDC sheath layers (Figure S5). The nitrogen adsorption–desorption isotherms of the CNT/HDC nanostructures showed a hysteresis in the relative pressure range of 0.4–0.6, thus indicating the generation of mesopores, which is due to the removal of the silica layer from the CNT–IL–silica composites (Figure S6). The textural data of the samples are summarized in Table S2.

The electrocatalytic activities of the heteroatom-doped CNT/HDC core–sheath nanostructures and reference catalysts were evaluated using the rotating ring-disk electrode (RRDE) technique. Linear sweep voltammetry (LSV) polarization curves of the catalysts for the ORR, which were measured in KOH electrolyte (0.1M) at a rotating speed of 1600 rpm and a scan rate of 5 mV s^{-1}, are shown in Figure 2a. The LSV curve of the CNTs exhibited on-set and half-wave potentials at 0.82 V and 0.72 V (vs. RHE), respectively, and showed an unclear current plateau, which indicates that the systems operates far from efficient four-electron transfer. HDC, as well as a physical mixture of CNTs and HDC, also exhibited on-set and half-wave potentials that are similar to those of the CNTs. The formation of HDC sheath layers on the CNTs markedly improved ORR activity and kinetics; the on-set and half-wave potentials of the CNT/HDC nanostructures were significantly shifted towards positive potentials with well-defined plateaus (Figure 2a and Table S3), indicating the synergistic effect of hybridization between CNT cores and HDC sheath layers. The highest ORR activity was achieved with CNT/HDC-1000, followed by CNT/HDC-900 and CNT/HDC-800. The most active material, CNT/HDC-1000, displayed on-set and half-wave potentials at 0.92 V and 0.82 V, respectively, and a kinetic current density of 8.3 mA cm^{-2} at 0.8 V. This high activity of the CNT/HDC nanostructures compares favorably with that of a benchmark Pt/C catalyst, which showed on-set and half-wave potentials at 0.98 V and 0.85 V, respectively. The Tafel slopes for CNT/HDC nanostructures ranged from 65.1 to 68.1 mV per decade, and were comparable to that of Pt/C (62.3 mV per decade), which indicates that the ORR kinetics of the CNT/HDC

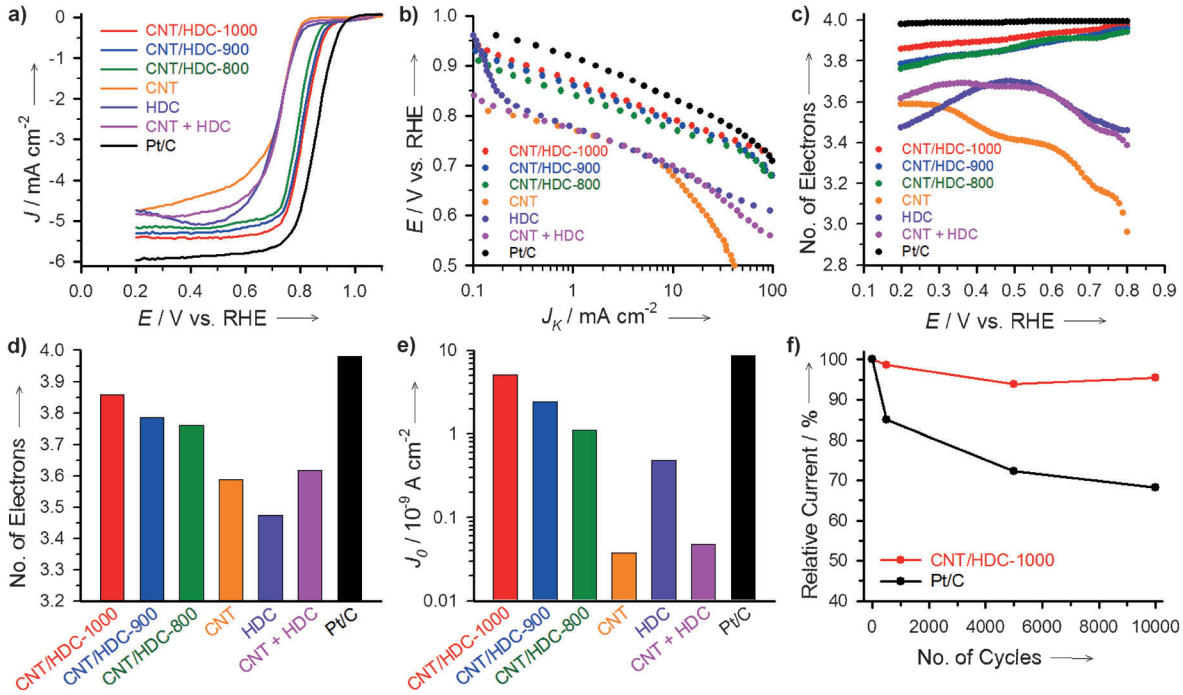

Figure 2. ORR activities and kinetics of the catalysts. a) LSV polarization curves and b) corresponding Tafel plots of catalysts for the ORR. c) Number of electrons that are transferred during the ORR versus potential. d) Comparison of the number of electrons that are transferred during the ORR at 0.2 V (vs. RHE). e) Comparison of exchange current densities of the catalysts. f) Long-term durability of the Pt/C and CNT/HDC-1000 catalysts for the ORR.

© 2014 Wiley-VCH Verlag GmbH & Co. KGaA, Weinheim

nanostructures are similar to those of Pt/C (Figure 2b). The number of electrons that are transferred by the CNT/HDC nanostructures was higher than for other samples and similar to that of the Pt/C catalyst, approaching four electrons over the entire potential range (Figure 2c,d). It is noteworthy that the exchange current density of the CNT/HDC-1000 sample approached that of Pt/C, and the values are of the same order of magnitude (Figure 2e). In contrast, the exchange current densities of the CNTs, HDC, and their mixture were one or two orders of magnitude lower than those of the CNT/HDC nanostructures and Pt/C.

We compared the ORR activity of the CNT/HDC nanostructure catalysts with that of doped CNTs (Figure S7). Nitrogen-doped CNTs were prepared by using ammonia or urea as the nitrogen source (see the Supporting Information for details), and the resulting catalysts were denoted as N–CNT–NH_3 and N–CNT–Urea, respectively. The two N–CNT catalysts showed better ORR activity and kinetics than undoped CNTs, which is consistent with previous results;[7,8] their activity, however, is inferior to that of CNT/HDC-1000. We also extensively compared the ORR activity and kinetics of CNT/HDC-1000 with those of previously reported doped nanocarbon catalysts. A comparison of the half-wave potentials and kinetic current densities (at 0.8 V vs. RHE) of these catalysts revealed the CNT/HDC nanostructure to be one of the best performing metal-free electrocatalysts for the ORR in basic media (Figure S8, S9 and Table S4).

Previous routes to doped carbon-based ORR catalysts required the judicious selection of precursors and experimental conditions for CVD or the use of toxic gases. In contrast, in our approach to CNT/HDC nanostructures, the formation of HDC sheath layers relies on a simple solution process followed by annealing under relatively mild conditions; therefore, this procedure is more amenable to large-scale syntheses. Furthermore, by choosing suitable ILs, the type and quantity of the heteroatoms in the HDC layers could be easily controlled. As demonstrated by the ORR activity and kinetics data, the CNT/HDC nanostructures show very high electrocatalytic activity for the ORR, surpassing that of doped CNTs and of previously reported catalysts. In the CNT/HDC nanostructures, the CNT cores could enable the efficient transport of electrons, while the thin HDC sheath layers, which are doped with numerous heteroatoms, may provide catalytically active sites. In particular, the presence of multiple dopants (N, S, and F) in the sheath layers could further enhance ORR activity, in accordance with recent reports that revealed an enhanced ORR activity for dual-doped carbon structures.[8,10]

We next investigated the durability of the catalysts. The changes in the current density percentages for the ORR at 0.85 V with cycling between 0.6 and 1.0 V clearly reveal that the durability of CNT/HDC-1000 is superior to that of the Pt/C catalyst (Figure 2f). The initial current density of the CNT/HDC-1000 composites minimally decreased (4.5% after 10000 cycles), whereas that of Pt/C decreased substantially by 32%. Compare to Pt/C, the CNT/HDC nanostructures also showed superior tolerance towards potential catalyst poisons, such as methanol (Figure S10).

Finally, we tested whether CNT/HDC-1000 could be used as the cathode catalyst in an alkaline fuel cell. The polarization and power density curves of the membrane electrode assemblies (MEAs) that employed CNT/HDC-1000 as a cathode catalyst are shown in Figure 3 . For comparison, CNTs

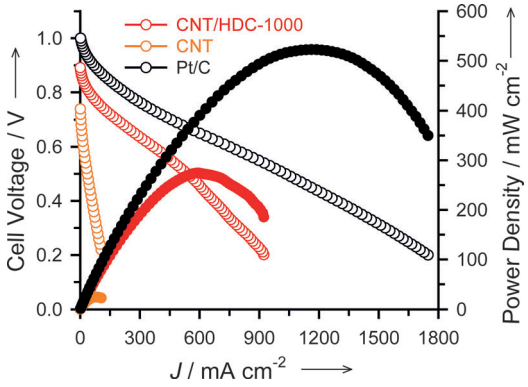

Figure 3. Performance of MEAs that employ CNT/HDC-1000, CNTs, or Pt/C as the cathodes in alkaline fuel cells at 50°C; open and closed circles correspond to cell voltages and power densities, respectively.

and Pt/C were also tested as cathode catalysts for alkaline fuel cells. The polarization curve of the CNT/HDC-1000-based MEA showed a very high on-set potential at 0.85 V, which is consistent with the ORR polarization curve that was obtained for the half-cell configuration. It is evident that the performance of the CNT/HDC-1000-based MEA is significantly better than that of the CNT-based MEA. At 0.6 V under H_2/O_2 operation, the CNT/HDC-1000 cathode generated current and power densities of 368 mA cm^{-2} and 221 mW cm^{-2}, respectively, which are 23.3 times higher than those of the CNT-based cathode. The performance of the CNT/HDC-1000 cathode is also substantially better than that of previously reported nitrogen-doped CNTs in an alkaline single cell (33.7 mA cm^{-2} and 20.2 mW cm^{-2}).[13] It is noteworthy that the performance of the CNT/HDC-1000-based MEA compares favorably with that of a Pt/C-based MEA. Therefore, the very high ORR activity of the CNT/HDC nanostructure was also demonstrated for a single-cell configuration.

In summary, we have developed an IL-driven, facile, scalable route to metal-free ORR electrocatalysts that are based on CNT/HDC core–sheath nanostructures. The CNT/HDC nanostructures showed excellent electrocatalytic activity and kinetics for the ORR, which is one of the best performances among metal-free, heteroatom-doped nanocarbon catalysts and compares favorably with that of the Pt/C catalyst. Furthermore, the durability and the tolerance towards methanol of the CNT/HDC nanostructures were superior to those of Pt/C. Importantly, the high ORR activity of CNT/HDC core–sheath nanostructures was translated to alkaline fuel cells. The design of core–sheath structures can be further applicable to other conductive core materials, such as graphene. Moreover, the use of metal-free CNT/HDC catalysts can be extended to other electrocatalytic and heterogeneous catalytic reactions.

© 2014 Wiley-VCH Verlag GmbH & Co. KGaA, Weinheim

Received: August 16, 2013
Revised: December 16, 2013
Published online: February 19, 2014

Keywords: carbon nanotubes · electrocatalysts · fuel cells · ionic liquids · oxygen reduction

[1] a) H. A. Gasteiger, S. S. Kocha, B. Sompalli, F. T. Wagner, *Appl. Catal. B* **2005**, *56*, 9; b) M. K. Debe, *Nature* **2012**, *486*, 43.
[2] P. G. Bruce, S. A. Freunberger, L. J. Hardwick, J.-M. Tarascon, *Nat. Mater.* **2012**, *11*, 19.
[3] a) S. Guo, S. Zhang, S. Sun, *Angew. Chem.* **2013**, *125*, 8686; *Angew. Chem. Int. Ed.* **2013**, *52*, 8526; b) K. Sasaki, H. Naohara, Y. Choi, Y. Cai, W.-F. Chen, P. Liu, R. R. Adzic, *Nat. Commun.* **2012**, *3*, 1115.
[4] a) M. Lefèvre, E. Proietti, F. Jaouen, J.-P. Dodelet, *Science* **2009**, *324*, 71; b) G. Wu, K. L. More, C. M. Johnston, P. Zelenay, *Science* **2011**, *332*, 443.
[5] J. Y. Cheon, T. Kim, Y. Choi, H. Y. Jeong, M. G. Kim, Y. J. Sa, J. Kim, T.-H. Yang, K. Kwon, O. Terasaki, G.-G. Park, R. R. Adzic, S. H. Joo, *Sci. Rep.* **2013**, *3*, 2715.
[6] Y. Zheng, Y. Jiao, M. Jaroniec, Y. Jin, S. Z. Qiao, *Small* **2012**, *8*, 3550.
[7] a) K. Gong, F. Du, Z. Xia, M. Durstock, L. Dai, *Science* **2009**, *323*, 760; b) S. Wang, D. Yu, L. Dai, *J. Am. Chem. Soc.* **2011**, *133*, 5182; c) L. Yang, S. Jiang, Y. Zhao, L. Zhu, S. Chen, X. Wang, Q. Wu, J. Ma, Y. Ma, Z. Hu, *Angew. Chem.* **2011**, *123*, 7270; *Angew. Chem. Int. Ed.* **2011**, *50*, 7132.
[8] a) S. Wang, E. Iyyamperumal, A. Roy, Y. Xue, D. Yu, L. Dai, *Angew. Chem.* **2011**, *123*, 11960; *Angew. Chem. Int. Ed.* **2011**, *50*, 11756; b) Y. Zhao, L. Yang, S. Chen, X. Wang, Y. Ma, Q. Wu, Y. Jiang, W. Qian, Z. Hu, *J. Am. Chem. Soc.* **2013**, *135*, 1201.
[9] a) L. Qu, Y. Liu, J.-B. Baek, L. Dai, *ACS Nano* **2010**, *4*, 1321; b) Z.-H. Sheng, L. Shao, J.-J. Chen, W.-J. Bao, F.-B. Wang, X.-H. Xia, *ACS Nano* **2011**, *5*, 4350.
[10] a) S. Wang, L. Zhang, Z. Xia, A. Roy, D. W. Chang, J.-B. Baek, L. Dai, *Angew. Chem.* **2012**, *124*, 4285; *Angew. Chem. Int. Ed.* **2012**, *51*, 4209; b) J. Liang, Y. Jiao, M. Jaroniec, S. Z. Qiao, *Angew. Chem.* **2012**, *124*, 11664; *Angew. Chem. Int. Ed.* **2012**, *51*, 11496.
[11] a) R. Liu, D. Wu, X. Feng, K. Müllen, *Angew. Chem.* **2010**, *122*, 2619; *Angew. Chem. Int. Ed.* **2010**, *49*, 2565; b) W. Yang, T.-P. Fellinger, M. Antonietti, *J. Am. Chem. Soc.* **2011**, *133*, 206; c) D.-S. Yang, D. Bhattacharjya, S. Inamdar, J. Park, J.-S. Yu, *J. Am. Chem. Soc.* **2012**, *134*, 16127.
[12] a) S. Yang, X. Feng, X. Wang, K. Müllen, *Angew. Chem.* **2011**, *123*, 5451; *Angew. Chem. Int. Ed.* **2011**, *50*, 5339; b) Y. Zheng, Y. Jiao, J. Chen, J. Liu, J. Liang, A. Du, W. Zhang, Z. Zhu, S. C. Smith, M. Jaroniec, G. Q. Lu, S. Z. Qiao, *J. Am. Chem. Soc.* **2011**, *133*, 20116; c) K. Kwon, Y. J. Sa, J. Y. Cheon, S. H. Joo, *Langmuir* **2012**, *28*, 991.
[13] C. V. Rao, Y. Ishikawa, *J. Phys. Chem. C* **2012**, *116*, 4340.
[14] a) X. Wang, S. Dai, *Angew. Chem.* **2010**, *122*, 6814; *Angew. Chem. Int. Ed.* **2010**, *49*, 6664; b) J. P. Paraknowitsch, J. Zhang, D. Su, A. Thomas, M. Antonietti, *Adv. Mater.* **2010**, *22*, 87.
[15] T. Fukushima, A. Kosaka, Y. Ishimura, T. Yamamoto, T. Takigawa, N. Ishii, T. Aida, *Science* **2003**, *300*, 2072.

© 2014 Wiley-VCH Verlag GmbH & Co. KGaA, Weinheim